ID 100

Tip Vortex Aperiodicity Correction: Removing Systematic Uncertainty in Core Radius due to Random Uncertainty in Position

Mahendra J. Bhagwat[a,*], Manikandan Ramasamy[b]

[a]*Research Scientist, US Army Aeroflightdynamics Directorate (AMRDEC), Ames Research Center M/S 215-1, Moffett Field, CA 94035, USA*
[b]*Research Scientist, UARC/ AFDD, NASA Ames Research Center M/S 215-1, Moffett Field, CA 94035, USA*

Abstract

Methods to correct for the effects of vortex wandering or aperiodicity were examined in the context of PIV measurements on rotor tip vortices. Unless corrected, the uncertainty in vortex center location (random motion of vortices about the mean) can introduce additional uncertainty in vortex properties derived from the measured velocity field. For example, the vortex core size derived from averaged or mean flow field appears larger because of aperiodicity. While correcting for aperiodicity is important, it is also important to understand the role played by the methods used to derive the vortex properties of interest in the resulting uncertainty. Global methods, which use a large extent of measured data, are shown to give smaller uncertainty in vortex properties compared to local methods, which use only a small sub-set of data close to the vortex core. The proposed new method is based on a planar least-squares fit and is global in nature. It also has the capability to include additional flow features such as a second vortex or a vortex sheet. The results clearly demonstrate this advantage in the form of smaller variation in the estimated core properties, even in the presence of secondary vortical structures, and also from the self-consistent results obtained using three different aperiodicity correction methods. The general applicability of the method is demonstrated using previous measurements from the TRAM and HART II tests.

Keywords: tip vortex, vortex aperiodicity, wandering, meandering, PIV, uncertainty

1. Introduction

Over the last decade particle image velocimetry (PIV) has found increasing use in rotor flow field and tip vortex measurements, and with great success. The applications have spanned a wide range from very large-field [1] to microscopic [2, 3] measurements. As the PIV measurement resolution increases, attention is again focused on understanding the associated measurement uncertainties. Perhaps a unique contributor to uncertainty in tip vortex measurements is their wandering or meandering motion; this is a seemingly random movement of the vortex center location normal to the vortex axis. For rotor tip vortices, this is often referred to as aperiodicity because the wandering motion appears as variation in vortex center location from one rotor revolution (period) to another. Several measurements must be averaged to obtain mean flow quantities and, in turn, mean vortex properties. Therefore, vortex wandering introduces uncertainty in the averaged flow quantities, and can potentially increase the resultant measurement uncertainty in vortex core radius and peak swirl velocity. In particular, the wandering motion results in a larger apparent core radius and a smaller peak swirl velocity.

Measurement uncertainty refers to an estimate of error bounds in the measurement. The two types of uncertainties are systematic uncertainty and random uncertainty. The first is sometimes called measurement bias and reflects measurement offsets. Systematic uncertainty is typically quantified using calibration and specially designed measurements. For PIV measurements, there has been significant work done to minimize or eliminate the systematic uncertainty – see, e.g., [4]. The current work does not address these uncertainties but instead focuses only on the random errors in the derived vortex properties, i.e., on random uncertainty.

Several measurements (derivations) of a quantity can provide a statistical estimate of the random measurement uncertainty. This is specified as a mean value with a confidence interval. The standard deviation represents a 68% confidence interval, i.e., the probability that a new measurement will fall within one standard deviation from the mean is 68%. Similarly, about two standard deviations corresponds to a 95% confidence interval. Alternatively, the uncertainty in a derived quantity can be estimated or predicted *a priori* using propagation of uncertainty in the measured quantities. The propagation of uncertainties can be very challenging to model. For example, vortex wandering is the uncertainty in the vortex center location and is often quantified in terms of the standard deviation normalized by the vortex core size. However, this random uncertainty in vortex location can cause a systematic uncertainty in vortex core radius (or peak swirl velocity) — the apparent core radius is larger, and this discrepancy increases with increasing vortex wandering. Clearly, there is need to correct for such uncertainty and several methods have been developed for aperiodicity correction.

Vortex aperiodicity or wandering is a particularly formidable problem for point measurement techniques like hot-wire anemometry (HWA) or laser Doppler velocimetry (LDV) where an averaged flow field can only be constructed by independently averaging measurements at each point. Using this "simple average," the wandering motion also contributes to velocity fluctuations at a fixed location, which may be mistaken for turbulence. One of the earliest attempt to assess the effect of wandering on tip vortex core properties is reported by Baker et al. [5]. This ef-

☆Presented in the aerodynamics session at the 37th European Rotorcraft Forum, Sept. 13–15, 2011.

*Corresponding author

Email addresses: mahendra.bhagwat@us.army.mil (Mahendra J. Bhagwat), mani.ramasamy@us.army.mil (Manikandan Ramasamy)

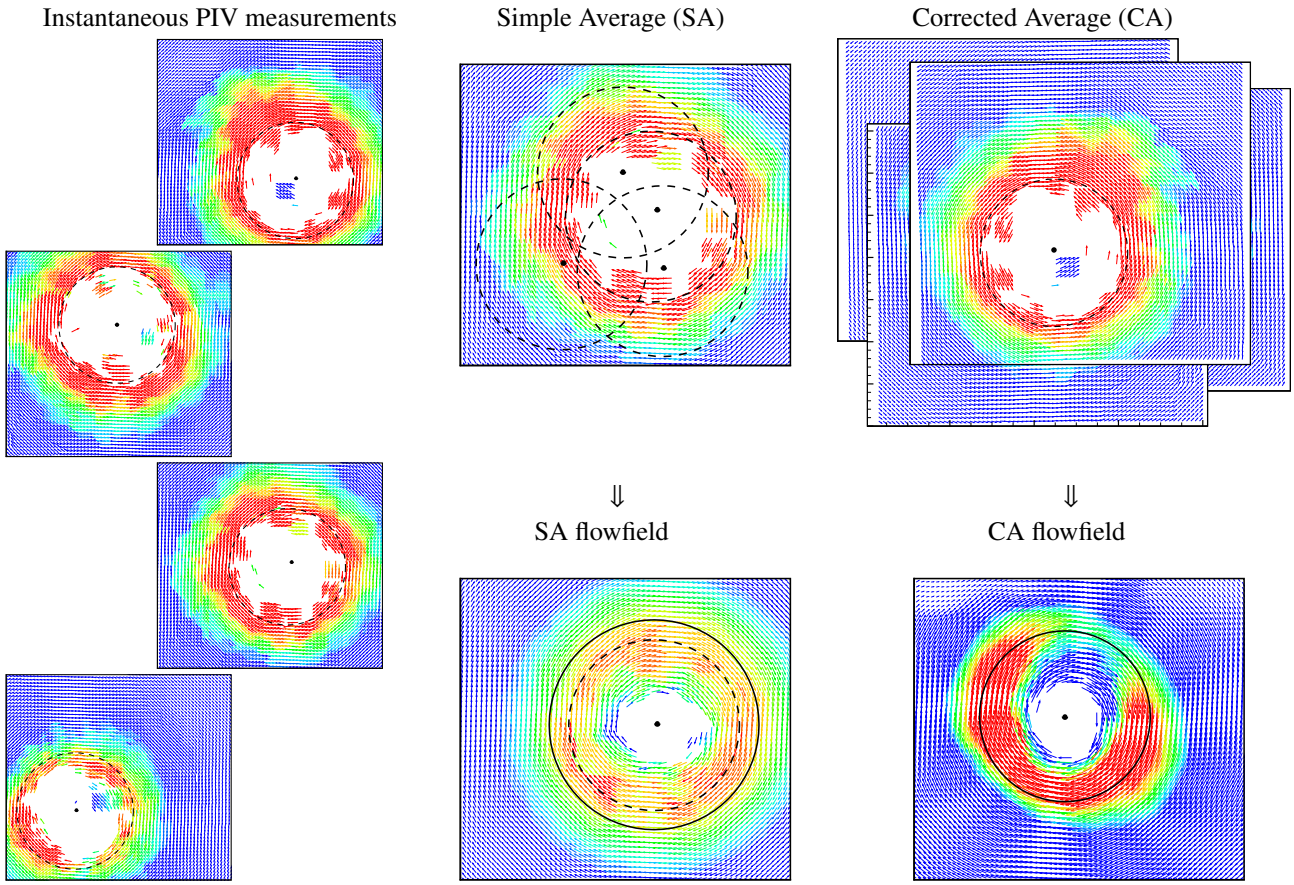

Figure 1: Schematic showing simple average and corrected average using a few sample PIV vector fields. The simple average gives a larger core size than the original samples, whereas the corrected average gives nearly the same core size.

fect can be eliminated by conditional sampling [6] or must be corrected using some measure of the vortex wandering. Devenport et al. [7] present an analytic correction procedure based on measured wandering magnitude. Leishman [8] presents a numerical correction procedure, similar to Devenport's analytic correction, for measured vortex velocity profiles.

Planar measurement techniques like PIV present other alternatives to help mitigate the effect of vortex aperiodicity. One of the earliest measurements on rotor tip vortices is presented in [9] for the TRAM rotor, where the aperiodicity correction procedure is also described in detail. The procedure is similar in spirit to conditional sampling where only a small set of samples with the vortex centers close together are chosen. Tee individual samples are aligned using their respective vortex centers prior to averaging, i.e., the measurements are "corrected" for the movement of vortex center location before averaging — hence the name corrected average. Unlike point measurement techniques, PIV allows one to obtain the vortex core properties from each individual plane measurement (image) as well. The average of these individual measurements would also be representative of mean vortex properties.

To better understand these aperiodicity correction methods, examples of simple average and corrected average are shown in Fig. 1. Individual measurements are shown as velocity vector field colored with velocity magnitude, with red being the highest and the black being the smallest velocity. For visualization purposes, the vortex center is shown with filled circle symbols and the approximate vortex core boundary, corresponding to the local maxima in swirl velocity, is marked with a circle. The vortex core is seen as a data void because of the difficulty in seeding the flow inside the core. Large variations in the vortex center location are readily apparent even in these four instances. When a number of such individual images are averaged to obtain mean flow properties, the resulting flow field is smeared because of the variation in the vortex center location. This is clearly seen in the simple average flow field, where the vortex appears larger in size, with lower swirl velocity, than any of the instantaneous measurements (shown by dotted lines).

An intuitively better approach for obtaining the mean flow characteristics is to first align the instantaneous measurements using their respective vortex centers — see Fig. 1. In this case, the averaging does not produce the smearing effect seen with simple average. In the corrected average flow field, the vortex looks nearly the same size as the instantaneous measurements. This is the central idea of the corrected average or conditional average for aperiodicity correction. The third method is the individual average, which does not "correct" the individual measurements for aperiodicity. Instead, the vortex properties are derived from each instantaneous measurement and then averaged to give mean vortex properties. This also readily provides an estimate of measurement uncertainty in terms of mean and standard-deviation of the desired vortex property.

Ideally, any of these methods, simple average, corrected average or individual average, should be equally effective. However, in [9] the average of individual vortex measurements was found to be significantly different from the "corrected" average obtained from the aligned individual measurements. This was attributed to large scatter in the individual vortex properties, i.e., to measurement uncertainty. Later experiments on a model scale rotor [10] and on the HART II rotor [11] also show such discrepancy between averaged individual measurements and corrected average profiles. One motivation for the current

work is to better understand and minimize these inconsistencies and how they affect the measurement uncertainties.

To minimize measurement uncertainty in vortex properties it is important to understand its sources. The underlying experimental uncertainty in the velocity measurements itself is outside the scope of the current work. However, the choice of analysis method is important in controlling the propagation and amplification of this uncertainty into derived quantities of interest like the vortex core size, circulation, etc. Determining the vortex center from the velocity field is an important first step for the corrected average process. van der Wall & Richard [12] suggest that a convolution-based method improved the accuracy of vortex center identification and resulted in reduced scatter in the derived vortex properties of interest. This claim is explored further in this paper, and the improvement in the final measurement uncertainty in vortex properties resulting from the vortex center identification method is examined. Note that while vortex aperiodicity can be a big contributor to the uncertainty in the derived vortex properties, the methods used to derive those properties can also play a very significant role.

The current work briefly reviews various methods for determining the vortex center and other properties of interest, and how the methods can potentially affect the final uncertainty. The aperiodicity correction removes a systematic uncertainty in the vortex core radius (and peak swirl velocity). However the analysis method determines how the random uncertainty propagates to the derived quantity. It is important to ensure that the method does add/amplify random uncertainty which may mask the benefits of aperiodicity correction. A new method based on a planar least-squares fit is proposed for obtaining both the vortex center and other vortex properties of interest. This method is shown to give reduced uncertainty in derived quantities like vortex core radius, circulation, etc. Furthermore, with the planar fit method the three aperiodicity correction methods give self-consistent results. The method is first demonstrated using model-rotor tip vortex measurements [3] and then extended to other measured flow fields including the TRAM rotor measurements [9] and the HART II measurements [11].

2. Methodology

In this section various methods for aperiodicity correction are reviewed, followed by methods to determine the vortex properties. These latter methods are categorized into local and global methods based on the spatial extent of the data used. The global methods are assumed to be inherently better because they use more measured data, while the local methods rely more on a smaller subset of data.

2.1. Aperiodicity correction

As described in the introduction there are three categories of aperiodicity correction methods: the simple average (SA), the corrected average or conditional average (CA), and the individual average (IA). Figure 2 shows these three methods and identifies key steps involved in each. The SA can be traced back to fixed-point measurement techniques like LDV/HWA, where only a simple average is possible. In this case, the measurements must be later corrected for the aperiodicity using empirical semi-analytic techniques – see [7] and [8]. In the current work the analytic expression given by Devenport et al. [7] is used to correct the core radius obtained using simple average. It must be noted that such correction is valid only when the aperiodicity magnitude (standard deviation in center location) is not larger than the core radius.

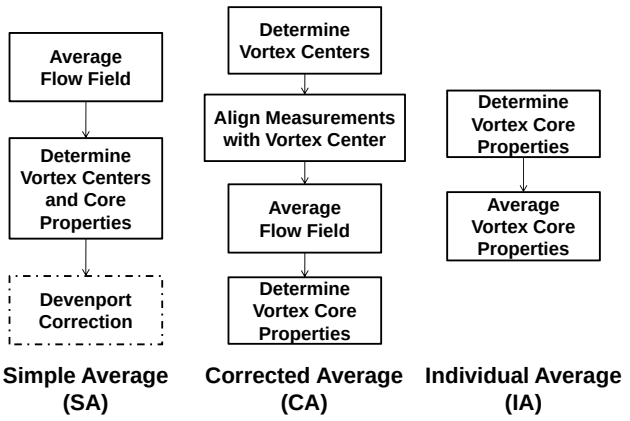

Figure 2: Tip vortex aperiodicity correction methods

The corrected average and individual average are possible only with a field measurement technique like PIV, and can be computationally intensive. However, these are applicable even with arbitrarily large aperiodicity magnitude. The third method, IA, has its advantages in simplicity; no flow field averaging is required and only the vortex properties derived from each individual (instantaneous) measurement are averaged. This also provides an estimate of measurement uncertainty in the form of mean, μ, and standard-deviation, σ, of each vortex property of interest, i.e., the measured property has a 68% confidence level in the $\mu \pm \sigma$ interval. All aperiodicity correction methods belong to one of these three categories, and differ only in their implementation details like the method for determining the vortex center and/or other vortex properties.

The choice of methods for determination of vortex core properties from either the averaged or the instantaneous flow field is independent of the aperiodicity correction. For the CA method, the vortex center for each individual measurement must be determined prior to determining the vortex core properties from the averaged flow field. For SA, the subsequent correction, like the Devenport correction, also needs the vortex center locations (aperiodicity magnitude). In fact, the accurate estimation of the vortex center is necessary for the accurate estimation of the vortex core properties [12]. These methods are divided into two categories, local methods and global methods. As the names suggest, the "local" methods are based on the flow field in close vicinity of the vortex center while the "global" methods are based on a larger flow field surrounding the vortex. It should be noted that the global/local categorization is not very rigid; it is simply the means to explain the observed differences in these methods.

2.2. Methods to determine vortex center

The most common methods to calculate the vortex center from measured flow field are based on some flow invariant property like vorticity, λ_2, and Q-criterion, etc. Most, if not all, of these flow quantities have a local maximum at the vortex center — hence the name local methods. Commonly used local methods include the measurement grid node that carries the maximum value of vorticity [9, 10, 13, 14], helicity, axial velocity [15], or Q-criterion [12, 15]. Centroid or area center of vorticity [11, 15] has also been used to determine the vortex center. Ideally the vortex center defined by any of these criteria is the same. However, the vortex center estimates do not always

agree [10, 11]. One short-coming of all of these methods is that they rely mostly on measurements near the vortex core, where reliable measurements are difficult to make. This is because of the challenges in getting enough seed in the vortex core [16] and the higher turbulence levels near the vortex core boundary. As a result, the measurements near the vortex core have a lower signal to noise ratio (a result of higher fluctuations and fewer samples), and contribute to errors in the estimated vortex center location. Eliminating such measurements with low signal to noise ratio results in a data void near the vortex center, which will make application of local methods even more difficult.

For the model-rotor tip vortex measurements presented here, the strict signal-to-noise ratio limits imposed on the PIV data resulted in a large data void region around the vortex center, which was often as big as the vortex core. In such cases, a local method is obviously ruled out and a global method must be employed. One global method found in the rotorcraft literature is the convolution-based method in [12]; this showed improved accuracy in determining the vortex center. Although the measurements reported in [12] did not show a data void near the center, the results definitely demonstrated the benefit of using a larger measured flow field rather than only a few measurement points inside the vortex core.

2.3. *Methods to determine vortex properties*

Having determined the vortex center, the next step is to determine key vortex properties like vortex core radius, peak swirl velocity, circulation, etc. As with the vortex center, the methods to determine vortex properties can also be divided into local and global categories. In this case, the local methods are usually based on measurements along straight-line cuts through the vortex center, perhaps using the analysis techniques developed for LDV/HWA measurements, which were often made only along straight line(s) passing through the vortex. The peak swirl velocity along these cuts defined the vortex core radius and asymptotic value of circulation defined the vortex strength [9, 17]. These methods are considered local methods because the core radius and peak-swirl velocity are determined from a local maximum in velocity. A variation of this uses a linear curve fit (based on an assumed vortex model) to the data along a straight line [11, 18]. A global method based on a planar fit to the entire measurement plane (or a suitably large enough subset of that) was used in [12] with good success.

It seems intuitively obvious that a global method that uses a large amount of measured data would be better than local methods that use a very, very small subset confined to the vicinity of a local maxima (often including measurements with lower signal to noise ratio and excluding those with possibly higher signal to noise ratio). However, this hypothesis remains to be carefully examined. The planar fit is a global method that combines the two tasks (determine vortex center and other properties of interest) into a single planar least-squares fit to the entire measurement plane (all velocity data). The planar fit is similar to the convolution method in the sense that maximizing the convolution of measurements with an assumed distribution is, in principle, the same as minimizing the error between the measurements and an assumed distribution. The key difference is that the same fit is used to obtain both the vortex center and the vortex properties of interest, like core radius, circulation, etc.

2.4. *New method: planar least-squares fit*

The newly proposed method is based on a planar least-squares fit of the measured velocities to those given by an assumed vortex model. In general, the measurement plane is not normal to the vortex axis. Therefore, the vortex axis orientation relative to the measurement plane must be taken into account to correctly identify the vortex core properties. A transformation is required between the measurement coordinate system (x, y, z) and the vortex coordinate system, (x_v, y_v, z_v). The vortex axis is aligned with the z_v-axis and positive circulation, Γ_v, is defined by the right-hand-rule. In the initial analysis only a swirl velocity model is used and is defined as a function of the radial distance, r_v, from the vortex center, along with a core radius, r_c, and the vortex circulation, Γ_v. This can, however, be easily extended to include all three vortex induced velocity components.

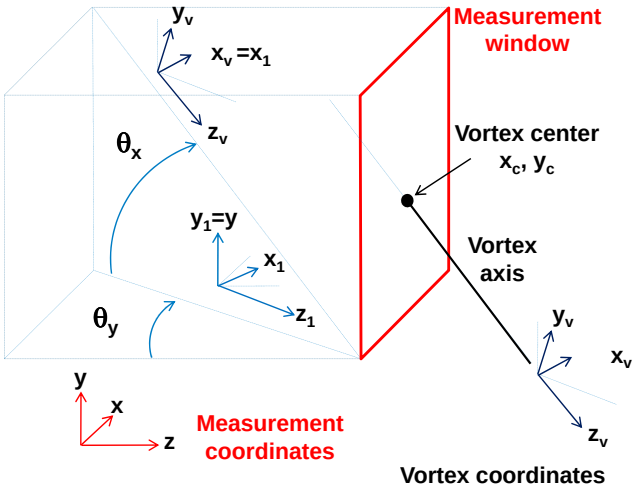

Figure 3: Inclination of vortex axis included through vortex convection velocities

The center of the vortex (x_c, y_c) is defined in the measurement coordinates, (x, y, z). The vortex convection velocity or background velocity is represented by (u_c, v_c), also in the measurement coordinates. Two rotation angles are required for the transformation from the measurement coordinates to the vortex coordinates. This is schematically shown in Fig. 3 where the PIV measurement window is shown along with the measurement and vortex coordinates. A first rotation of θ_y around the y-axis results in an intermediate coordinates (x_1, y_1, z_1) and a subsequent rotation θ_x around the x_1-axis gives the vortex coordinates. The transformation matrices are given by

$$R_y = \begin{bmatrix} \cos\theta_y & 0 & -\sin\theta_y \\ 0 & 1 & 0 \\ \sin\theta_y & 0 & \cos\theta_y \end{bmatrix} \quad (1)$$

$$R_x = \begin{bmatrix} 1 & 0 & 0 \\ 0 & \cos\theta_x & \sin\theta_x \\ 0 & -\sin\theta_x & \cos\theta_x \end{bmatrix} \quad (2)$$

The transformation from the measurement coordinates to the vortex coordinates is then given by

$$\begin{Bmatrix} x_v \\ y_v \\ z_v \end{Bmatrix} = [R_x]\left[R_y\right]\begin{Bmatrix} x - x_c \\ y - y_c \\ z \end{Bmatrix} \qquad r_v = \sqrt{x_v^2 + y_v^2} \quad (3)$$

The vortex swirl velocity is transformed to the Cartesian vortex coordinates as

$$\begin{aligned} u_v &= -V_\theta \sin\theta = -V_\theta \frac{y_v}{r_v} \\ v_v &= V_\theta \cos\theta = V_\theta \frac{x_v}{r_v} \end{aligned} \quad (4)$$

These velocities are then transformed back to the measurement coordinates using the inverse transform. The resulting function for the vortex velocity field is given by

$$\mathbf{f}\left(r_c, \Gamma_v, x_c, y_c, u_c, v_c, \theta_x, \theta_y\right) =$$

$$V_\theta\left(r_v, r_c, \Gamma_v\right)\left[R_y\right]^T \left[R_x\right]^T \begin{Bmatrix} -\frac{y_v}{r} \\ \frac{x_v}{r} \\ 0 \end{Bmatrix} + \begin{Bmatrix} u_c \\ v_c \\ 0 \end{Bmatrix} \tag{5}$$

The least-squares fit uses the above function with the eight independent variables, viz., $r_c, \Gamma_v, x_c, y_c, u_c, v_c, \theta_x, \theta_y$, to obtain the best match with measured velocities.

To perform a least-squares fit to the function $\mathbf{f}$ as defined above, a suitable vortex velocity profile model for swirl velocity distribution must be chosen. The results shown in current work used the Lamb-Oseen model, i.e.,

$$V_\theta = \frac{\Gamma_v}{2\pi r}\left(1 - \exp\left(-\alpha\left(r/r_c\right)^2\right)\right) \tag{6}$$

where $\alpha = 1.25643$. The laminar Lamb-Oseen model is used in all the results presented here for several reasons. First and foremost, the data suggests that the vortex profile is nearly laminar even though the chord or vortex Reynolds numbers may suggest a turbulent vortex. Secondly, the Lamb-Oseen model has a simple closed-form expression and can be readily extended to three-dimensions using the Newman model [19]. It should, however, be noted that the planar fit can readily incorporate other vortex models. It was shown in [3] that the choice of vortex models did not affect the vortex center location. Each model gave a slightly different core radius corresponding to different values of core circulation to the final circulation ratio. For example, a potential vortex (or Rankine vortex) where all the circulation is contained inside the vortex core, a laminar Lamb-Oseen vortex [20, 21] where about 70% circulation is contained in the core, a fully turbulent model by Iversen [22] where only about 40% circulation is contained in the core, give progressively smaller core radius.

Another consideration is sub-grid analysis where a small sub-set of data is chosen around the vortex based on either the distance from the vortex center or threshold value of flow properties such as vorticity, e.g. [11]. The local methods for vortex center determination typically show some sensitivity to the size of the sub-grid surrounding the vortex. The planar fit, a global method, was shown in [3] to be essentially insensitive to sub-grid size. While the vortex center location obtained using different sub-grid sizes varied within 0.01% chord of each other, the vortex properties, like circulation and core radius, showed very low sensitivity to sub-grid size. In [3], the sensitivity to sub-grid size was used as a statistical filtering criteria such that the individual measurements that showed a difference of greater than 2% in vortex circulation between three sub-grid sizes were not included in the analysis. Only about 2–3% of the measurements did not meet this criterion. In the current work, therefore, the entire flow field data is used for the analysis unless otherwise stated.

The planar fit that uses a vortex model to fit the data gives sub-grid accuracy in the sense that the vortex center location is not constrained to coincide with a grid node, as would be the case if it was based on, for example, maximum vorticity. Similarly, the core radius is not constrained by the grid resolution as would be the case if it was based in peak swirl velocity locations. Therefore, the current work does not involve any re-meshing and/or interpolation of the measured data to a sub-grid. For the corrected average, the individual measurements are aligned using the measurement grid node closest to the vortex center determined using the planar fit. This, in effect, only reduces the aperiodicity in the tip vortex location, rather than eliminate it all together.

3. Results & Discussions

In this section the results obtained using the planar fit are shown for three different rotor tip vortex measurements. The first set of measurements is the model-scale rotor tip vortex measurements made at AFDD using microscopic-PIV [3] using highly-twisted tilt-rotor blades. Results at $C_T = 0.0076$ are shown at two vortex ages of 4 deg and 15 deg. Measurements were also made at zero thrust, where a tip vortex with negative strength (per usual conventions) was seen going above the rotor owing to the high negative blade twist. The second set of measurements are the TRAM rotor measurements originally reported by Yamauchi et al. [9] in 1999, and the final set of measurements is the HART II measurements at position 17, studied in detail by all the HART II partners, and summarized in [11].

3.1. AFDD model-rotor tip vortices

The measurements presented here were performed on a three-bladed model-scale rotor system with a highly-twisted rotor blade that was similar to the XV-15 blade. The blade had a radius of 656 mm and 49 mm chord and was operated at a tip speed of 55 m/s. Figure 4 shows a summary of all the vortex properties for the $C_T = 0.0076$, $\psi_v = 15$ deg case. Measurements at $\psi_v = 4$ deg show the same qualitative trends and are not shown. A map of vortex center locations, and the representative core size are shown in Fig. 4(a). Recall that the corrected average procedure used in the current work does not re-mesh and interpolate measurements after aligning the vortex centers. As a result, the corrected average does not *completely* eliminate the aperiodicity, but only reduces it to less than one grid cell. The grid lines correspond to the measurement grid and show the high resolution achieved using a microscope. The residual aperiodicity can be seen in Fig. 4(a) from the corrected vortex center locations. The distribution of vortex center locations x_c and y_c is shown in Fig. 4(b), which is suggestive of a Gaussian distribution. The Devenport correction is based on the deconvolution of a Gaussian wandering motion; the observed distribution suggests that such an analytic correction would indeed be applicable.

Figures 4(c) and (d) show the results for the vortex axis orientations, θ_x and θ_y, and the mean vortex convection velocities, u_c and v_c, respectively. The vortex core radius and circulation are shown in Figs. 4(e) and (f), respectively. All three aperiodicity correction methods give results consistent with each other for all vortex properties. For the core radius, in Fig. 4(e), the SA method gives a larger core radius as expected; the subsequent Devenport correction gives a core radius that closely agrees with the CA and IA results. Notice that in all cases the vortex properties show a roughly Gaussian distribution. The standard deviation in circulation and core radius is about 5% standard-deviation, relative to their respective mean values. The differences in vortex properties obtained using the three aperiodicity correction methods are smaller than the standard deviation. In this paper the random measurement uncertainty is quantified using the standard-deviation normalized with the mean $\left(\sigma/\mu\right)$,

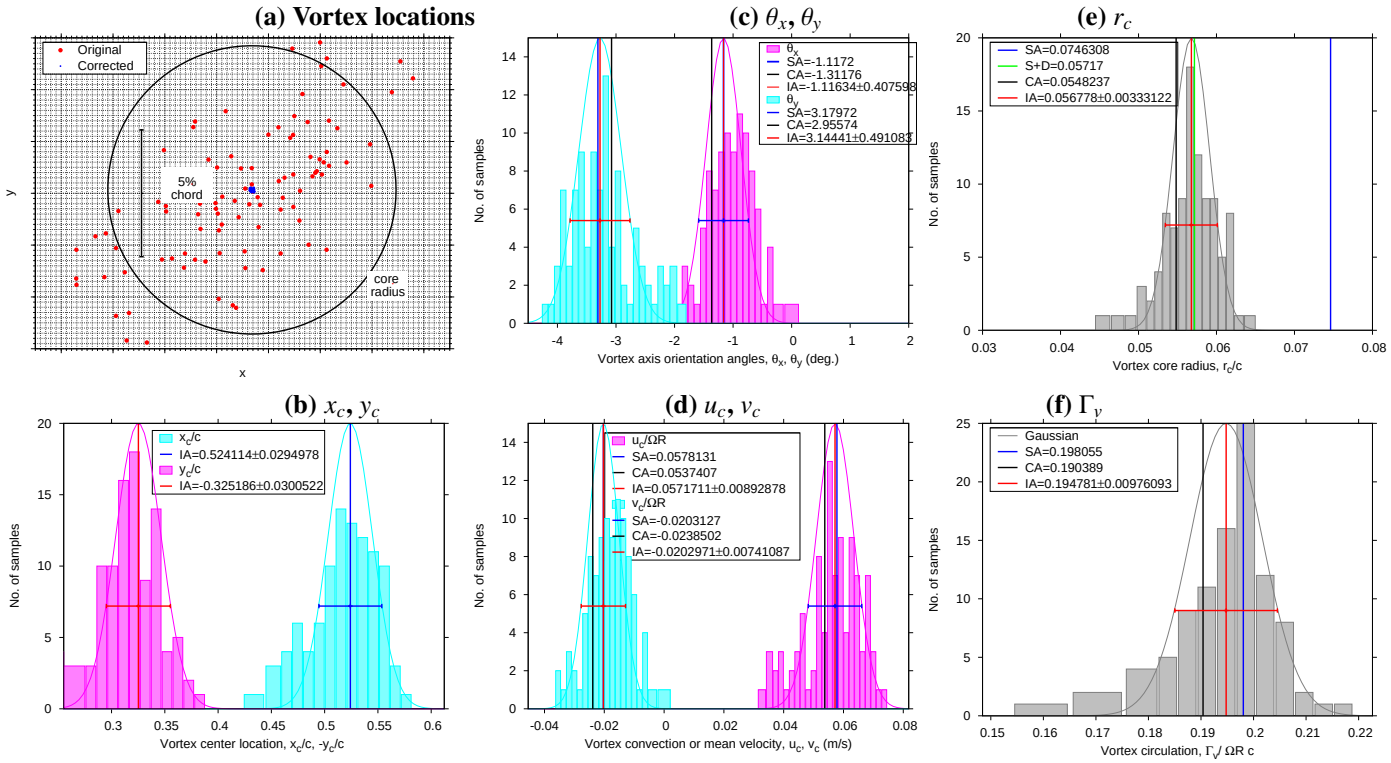

Figure 4: Example of vortex properties obtained using the planar fit for the AFDD model-rotor tip vortex measurements, $C_T = 0.0076$, $\psi_v = 15$ deg. Distribution of individual samples is shown as histograms along with the simple average, corrected average and individual values (mean and standard deviation) are shown. (a) Vortex center locations before and after center alignment, (b) Vortex center locations, x_c, y_c, (c) Vortex axis orientation angles, θ_x, θ_y, (d) Vortex convection velocities, u_c, v_c, (e) Vortex core radius, r_c, and (f) Vortex circulation, Γ_γ.

bearing in mind that the interval $\mu \pm \sigma$ corresponds to a 68% confidence level.

Figure 5 shows the measurement uncertainty in the vortex core radius and the vortex circulation, expressed as a percentage relative to the respective mean values. These are compared with results from three previously reported rotor tip vortex measurements: the UMD measurements from [17] for a small-scale rotor tip vortices; the TRAM measurements from [9] for the high thrust case; and the HART II measurements from [12] for the hover $\psi_v = 44$ deg case. The corresponding vortex aperiodicity magnitudes (standard deviation of vortex location normalized by core radius) are also shown for comparison. Interestingly, the two measurements with higher aperiodicity magnitudes showed lower resulting measurement uncertainties. It appears then that uncertainty must result from other factors like the measurement resolution. For tip vortex measurements, resolution is not compared as an absolute length scale, but relative to the vortex core being measured. The ratio of the measurement length (window size) to the core radius, i.e., l_m/r_c, has been used in the past as a measure of *relative* PIV resolution. This is schematically shown at the top of Fig. 5 with the squares representing the PIV processing window relative to the vortex core size shown by the circle. The current measurements have a significantly lower l_m/r_c ratio owing to the use of a microscopic lens. However, this appears to have played only a small part in the resulting measurement uncertainty. The UMD measurements have a small l_m/r_c ratio but a larger uncertainty, while the HART II measurements have a larger l_m/r_c ratio but a smaller uncertainty.

It must be reiterated that the uncertainty in derived quantities such as the vortex core radius, or circulation, is not simply experimental uncertainty. Instead the uncertainty is the result of the underlying experimental uncertainty in the velocity measurement propagated into the derived quantities, along with any

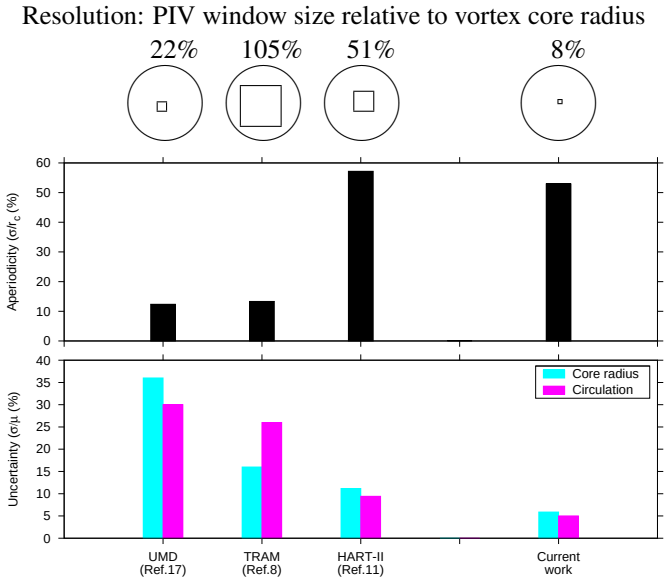

Figure 5: Measurement uncertainty in the vortex core radius and circulation compared for various experiments including the AFDD model-rotor measurements. The vortex aperiodicity magnitude (standard deviation normalized by vortex core radius) is also shown for all cases along with a schematic representation of the vortex core and the relative PIV window size.

additional uncertainty associated with the derivation method itself. Therefore, it is important to examine the methods used to derive these quantities of interest, and to ensure that their contribution to the resulting measurement uncertainty, over and above the underlying experimental uncertainty, is minimal. The analysis methods appear to have a role in the final perceived measurement uncertainty because one key difference between the four results shown in Fig. 5 lies in the analysis methods. The UMD and TRAM experiments used local methods for obtaining the vortex center and other vortex properties. The HART II results

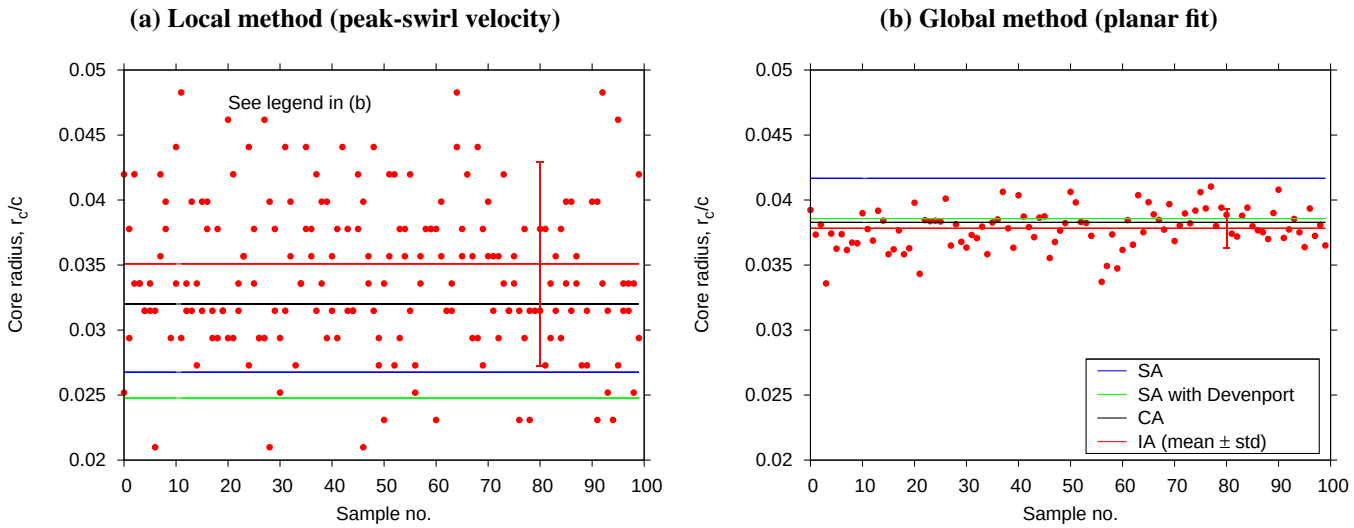

Figure 6: Vortex core radius for the AFDD model-rotor derived from the measured velocity field using (a) a local method (based on peak swirl velocity along horizontal/vertical cuts through the center), and (b) a global method (the planar fit based on least-squares fit). $C_T = 0.0076$, $\psi_v = 4$ deg.

(in particular, the results presented in this figure from [12]) used global methods; the vortex centers were obtained using a convolution of λ_2 and the vortex properties were obtained from a planar curve fit. The current work also uses a global method as described earlier. Figure 5 strongly suggests that using global methods for data analysis result in significantly lower measurement uncertainty in derived vortex properties. This working hypothesis can be tested in two ways: reanalyze the present measurements using a local method and reanalyze other measurements using the planar fit.

3.2. *Local method applied to the AFDD model-rotor measurements*

The model-rotor measurements were analyzed using a local method are shown in Fig. 6 for the case of $C_T = 0.0076$, $\psi_v = 4$ deg. In this case, the vortex center was first identified using the planar least-squares fit. The vortex properties were, however, not obtained from the fit. Instead, horizontal and vertical cuts were made through the vortex center, and the vortex core was identified using the peak swirl velocity locations along these cuts. The core radius was given by the distance between the peak swirl velocity and the vortex center. Similar cuts were made to the averaged flow fields using both SA and CA methods. These results are shown as a scatter plot in Fig. 6(b) with the core radius for each measurement sample along with the averaged values. The IA results show a significantly large scatter of about 23%, compared to those obtained using the least-squares fit shown in Fig. 6(b). The results obtained using only horizontal/vertical cuts also show inconsistencies — the SA core radius is much smaller than the CA result and the IA result. The local method clearly introduces a much larger uncertainty in the vortex core radius as compared to the global method.

The measurement uncertainty using the local and global methods is compared in Fig. 7 for the current measurements at $C_T = 0.0076$, $\psi_v = 4$ deg. As a small variation of this local method, the distance between two swirl velocity peaks on either side of the center was considered to be the core diameter. There is some cancellation of errors leading to slightly less uncertainty in the core radius as shown in Fig. 7. A similar behavior was observed earlier in Fig. 5. The UMD measurements [17] used the distance from the vortex center to the

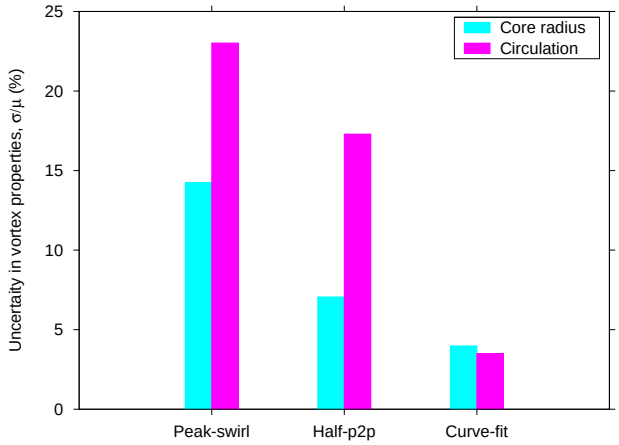

Figure 7: Effect of local and global methods on uncertainty $C_T = 0.0076$, $\psi_v = 4$ deg.

peak-swirl location as the vortex core radius. The TRAM results [9] used the distance between two opposite peaks as the core diameter. This observation reinforces the intuition that the analysis method used to derive the vortex properties adds to the perceived measurement uncertainty, with the local methods giving significantly larger uncertainty than the global methods.

Recall that the region near the vortex center is characterized by lower signal to noise ratio for the velocity measurements because of insufficient number of good data samples available there, suggesting that local methods would lead to larger uncertainties in the derived quantities than the global methods. To better understand why the local methods increase the measurement uncertainty, the horizontal/vertical cuts are examined further. If data with lower signal to noise ratio is removed, then there is a void near the vortex center. This data void may not always be symmetric relative to the vortex center — see Fig. 8(a). In this case, the derived core radius may be much larger than the underlying vortex. Alternately, the higher fluctuations in velocity near the vortex core may result in some spurious velocity measurements. Note that these measurements are not, strictly speaking, wrong, but are statistically incomplete due to lack of large enough samples. Such measurements may play a bigger role in determining the vortex properties using local methods. This problem is further exacerbated by the data void near such spurious measurements. For example, in Fig. 8(b) one spurious data point is seen to significantly alter the derived vortex core

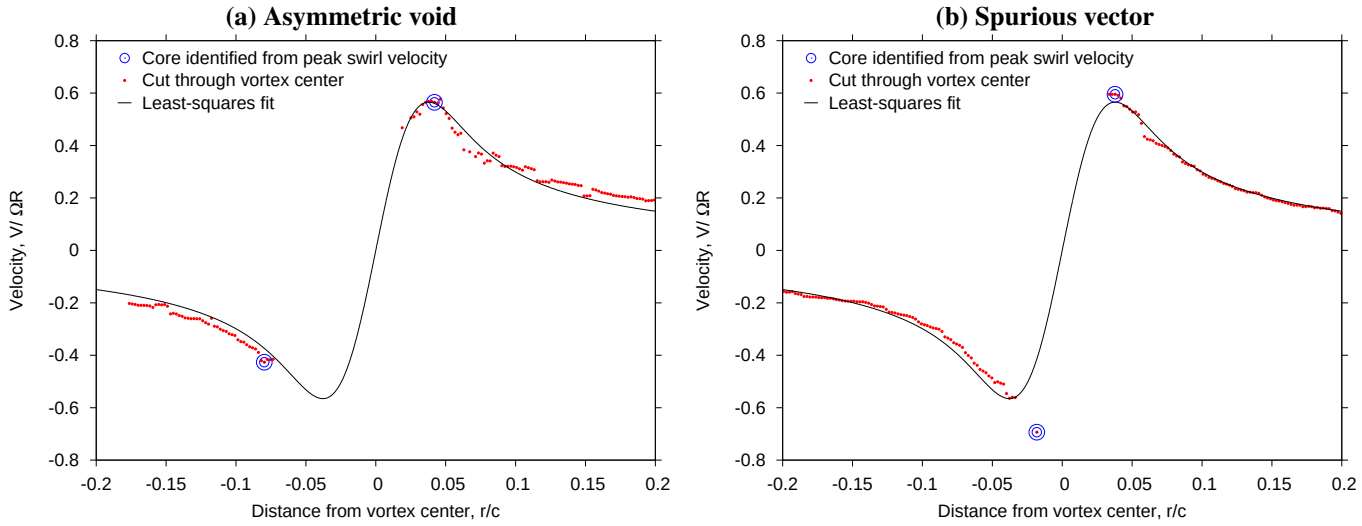

Figure 8: Examples showing the advantage of the least-squares fit in the presence of (a) asymmetric void, and (b) spurious measurements near the vortex center. $C_T = 0.0076$**,** $\psi_v = 4$ **deg.**

radius. Issues such as these contribute to the increased uncertainty in derived vortex properties obtained using local methods. Notice that in both Figs. 8(a) and (b) a curve-fit gives a better estimate of the vortex core, because it gives equal weight to data points further away — hence the name global — in determining the vortex properties and thereby limiting the impact of such errors.

Having reinforced the hypothesis that global methods for determining vortex center and vortex properties are better, the planar fit is applied to two of the previous measurements shown in Fig. 5 for additional confirmation.

3.3. TRAM measurements

The planar least-squares fit was applied to the TRAM results first reported in Ref. [9]. Two cases were considered: one high thrust case and one low thrust case, where two counter-rotating vortices were measured. The TRAM measurements are different from the hover measurements shown earlier and would challenge the planar fit. These are forward flight measurements and the PIV flow field shows large mean vortex convection velocities and larger vortex axis orientation angles. Results for the vortex core radius are shown in Fig. 9 as a scatter plot along with the respective SA, CA and IA values. Unlike the AFDD model-rotor hover measurements, shown in Fig. 6(b) for example, the TRAM measurements show a much larger scatter of about 15%. The averaged results were inconsistent with the CA showing a very large core size compared to the SA or IA values. The results for vortex circulation (not shown here) also showed similar inconsistencies, even larger in magnitude. Visualization of the measured flow field provided a clue for understanding these inconsistencies — one example is shown in Fig. 9(b) where the velocity vectors are shown with the contour colors representing the vorticity. The reason for the inconsistent results appears to be the presence of two vortices in the flow field, which can significantly influence the derived vortex properties.

The simple first step to correct this behavior is to remove the second vortex near the left hand bottom corner. This was done by only considering the right half of the image as shown by the dotted rectangle in Fig. 9(b). This was also the approach followed in [9] and, as a result, only one vortex was reported for this high thrust case. The results obtained using the planar fit with the smaller measurement window are shown in Fig. 10. Notice that the scatter is only slightly lower than the earlier results but now the three different methods SA, CA and IA agree closely with each other. As shown earlier in Fig. 5, the aperiodicity magnitude in this case was very small and the correction to SA does not change the core radius very much at all. This suggests that the planar fit can be applied to these measurements but some modifications are called for based on the flow field being studied.

The second case from the TRAM experiments was the low thrust case with two counter-clockwise vortices present in the flowfield. In this case, the vortices are much closer to each other, and it would not be possible to eliminate the effect of one vortex on the other by simply reducing the measurement window being considered. Instead, the least-squares fit was modified to include two vortices. This is easily done by modifying the fit function to include additional parameters corresponding to the second vortex, i.e.,

$$\mathbf{f}\left(r_{c_1}, \Gamma_{v_1}, x_{c_1}, y_{c_1}, \theta_{x_1}, \theta_{y_1}, r_{c_2}, \Gamma_{v_2}, x_{c_2}, y_{c_2}, \theta_{x_2}, \theta_{y_2}, u_c, v_c\right) \qquad (7)$$

The vortex core radii derived using this two-vortex fit are summarized in Fig. 11. The SA, CA and IA results are compared with those reported in [9]. Note that only one vortex for the high thrust case was reported in [9], whereas the current work includes results for both the vortices. As expected, the SA results are similar for the two methodologies but the CA results show a consistent behavior with the planar fit. The IA results for the planar fit show a much smaller standard deviation than the results from [9]. This again confirms the hypothesis that a global method results in a much smaller measurement uncertainty than a local method. This is best seen from Fig. 12 where the results are presented as uncertainty in vortex core and circulation measurements for both the previous and the current work. Again, the normalized standard deviation as a 68% confidence level is used as a measure of the uncertainty. This figure show the same effect as previously shown in Fig. 7 but with the TRAM measurements; the least-squares fit gives a much lower uncertainty than that obtained using peak vorticity for vortex center determination with half-peak-to-peak swirl velocity giving the core radius.

3.4. HART II measurements

The planar fit was also applied to the HART II measurements at position 17. This position has been studied in great detail by the HART II partners, and a comparative summary

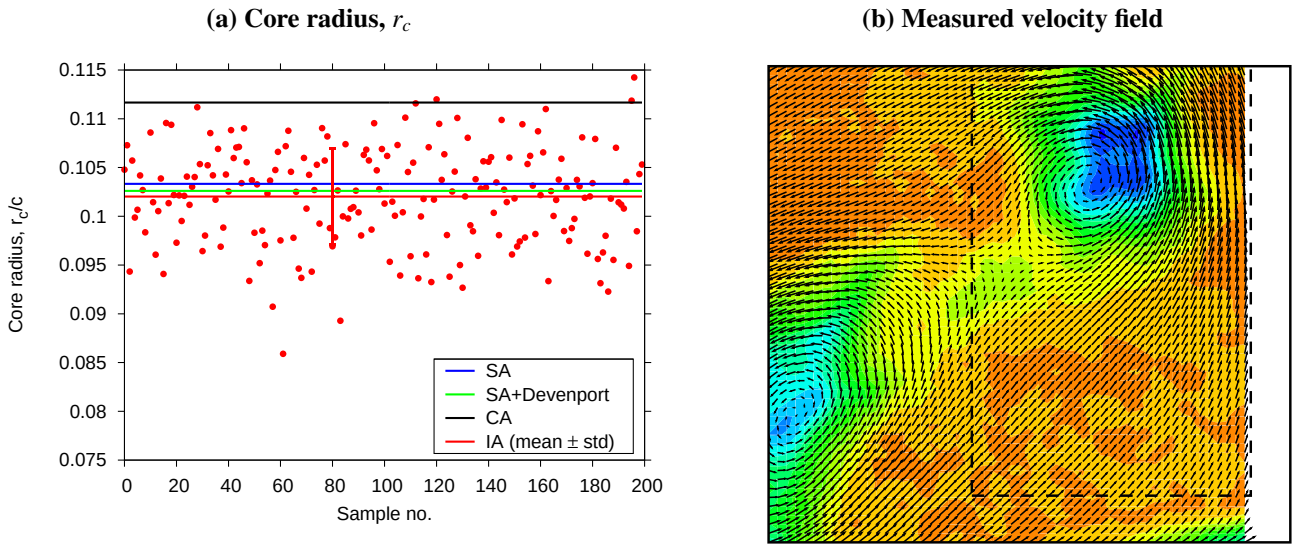

Figure 9: TRAM high thrust case: (a) Scatter plot of core radius for each individual sample shown with SA, CA and IA results. (b) Example flow field shows the presence of two vortices in the measurement window. Velocity vectors are shown along with contours of vorticity (blue positive, red negative). Dotted lines denote small region separately analyzed to isolate one vortex.

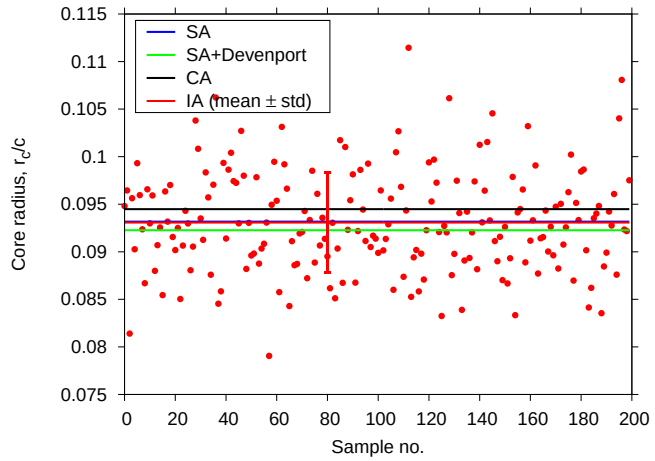

Figure 10: TRAM high thrust case: only half the flow field, shown by dotted lines in Fig. 9(b) is analyzed to exclude the vortex near the left hand bottom corner. Scatter plot of core radius is shown with SA, CA and IA results.

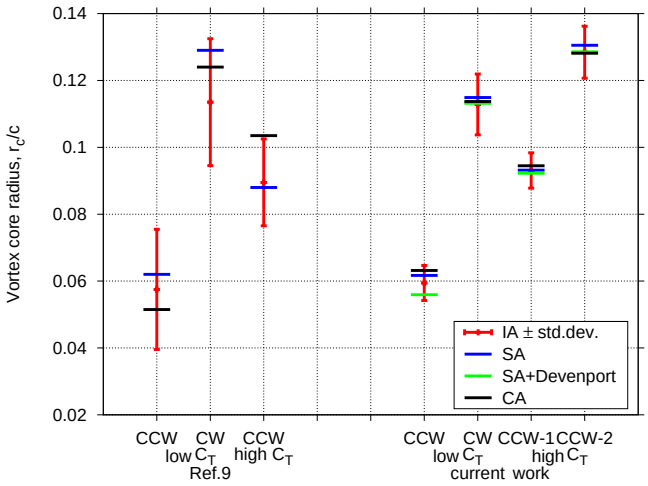

Figure 11: Core radius calculated from the flowfield using the planar fit compared with results presented in [9] (only one vortex was reported for the high thrust case). The results are shown as IA with standard-deviation together with CA and SA values. Current results include the Devenport correction with SA.

of analyses performed by US Army AFDD, DLR and ONERA are presented in [11]. An example flow field shown in Fig. 13

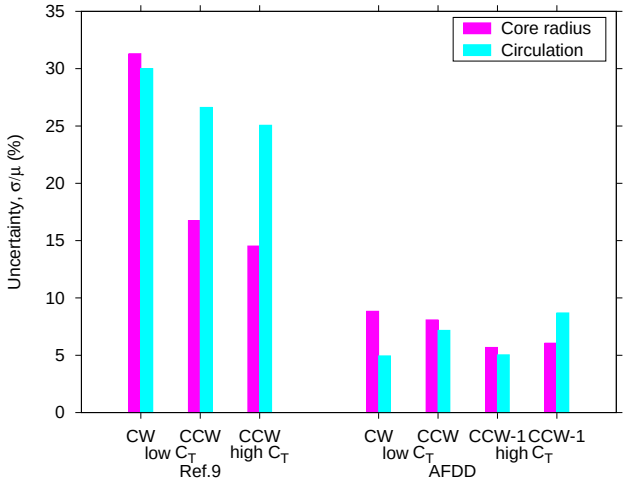

Figure 12: Measurement uncertainty in vortex core radius and circulation for the TRAM results using both the planar fit and the results reported in [9].

shows a relatively strong vortex sheet in close vicinity of the vortex core being examined. The presence of this vortex sheet is biasing the vortex center determined by the planar fit more toward the left. In this case the contours represent the velocity magnitude, and at least a part of the vortex core boundary can be clearly identified by the large swirl velocity region near the right-top corner.

The planar fit can be easily modified to account for the presence of a vortex sheet. The sheet appears like one half of a vortex with the other half stretched along the sheet length. A quick representation of such vortex sheet was devised using the Lamb vortex profile at the sheet edge (semicircular region), combined with the tangential velocity along the length of the sheet also given by the Lamb profile as a function of normal distance from the sheet. In the vortex sheet coordinates as shown in Fig. 13(b), with the vortex sheet extending along the negative x_s-axis, the sheet induced velocity field given by

$$\begin{aligned} x_s \geq 0 \quad & \text{Lamb vortex} \\ x_s \leq 0 \quad & u_s = \frac{\Gamma_s}{2\pi y}\left(1 - exp(-\alpha\frac{y^2}{r_s^2}\right), v_s = 0 \end{aligned} \tag{8}$$

The least-squares fit now includes the sheet location, circulation strength (γ_s), core radius (r_s) and orientation axes as additional parameters. Note that the sheet representation requires

(a) Measured flow field

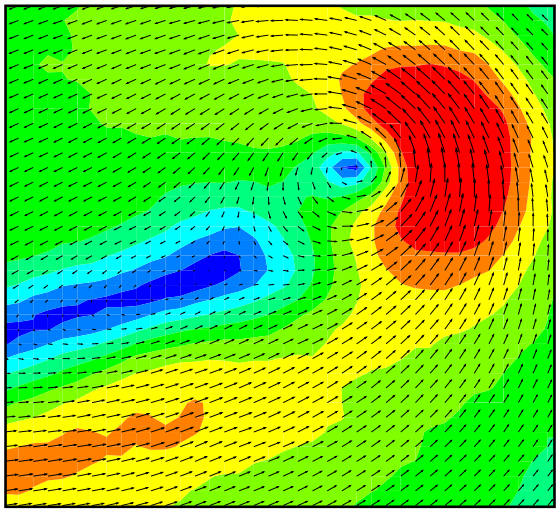

(b) Function fit including a vortex sheet

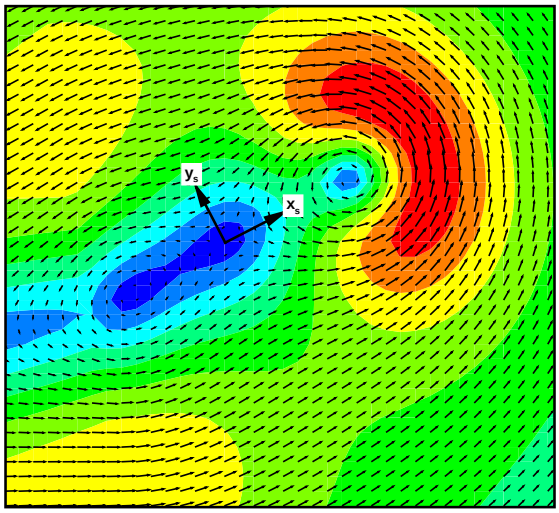

Figure 13: Simple average flow field for the HART II position 17 . (a) The measured flow field, (b) Function fit including a vortex sheet. Velocity vectors are shown along with contours of velocity magnitude, blue is the smallest and red is the largest.

one extra orientation angle to account for in-plane rotation of the sheet, as shown by the orientation of x_s, y_s-axes shown in Fig. 13(b). An example of the flow field given by such a functional representation is shown in Fig. 13(b) and appears to be a good representation of the measured flow field shown in Fig. 13(a), though the Lamb-vortex based model is certainly not the most appropriate functional representation of a vortex sheet. If the vortex sheet properties are also of interest, then a more appropriate function must be chosen. However, the simple representation used here certainly helps eliminate the effect of the sheet on vortex properties.

The importance of including the vortex sheet in the functional fit can be best understood by comparing the results with and without it. The core radius and vortex centers calculated by the planar fit without the vortex sheet are shown in Fig. 14 along with the results from different HART II partners. The individual vortex center locations using the planar fit, as well as those calculated by AFDD in [11] using the centroid of vorticity, are shown. The diamond symbols represent the vortex centers determined by various methods (AFDD, DLR, ONERA results from [11]), and the circles represent the vortex cores themselves; the core radius is the radius of the circle. The measurement grid is also shown to give an idea about the PIV resolution. All methods appear to pick this high velocity region as the vortex core boundary as suggested by Fig. 14, where the vortex cores calculated using different methods all line-up along this high swirl velocity region. The planar fit also identifies this region as the vortex core boundary. However, the vortex center is shifted to the left (compared to all other calculations) resulting in a larger core radius. The reason for this behavior is clearly the presence of the vortex sheet in close proximity to the vortex.

Table 1: Peak vorticity and orientation angles for HART II position 17

	Method/source	Vorticity, γ/Ω	θ_x	θ_y
[11]	AFDD	33.1	-0.7°	-19.4°
	DLR	30.8	4.3°	-19.2°
	ONERA	31.5	1.6°	-25.7°
Planar fit	CA	27.4	7.9°	-18.9°
	SA	25.2	7.7°	-22.2°
	SA+D	33.2		
	IA	33.9	-2.5°	-16.3°

The results are shown again in Fig. 15 using the modified methodology that accounts for the vortex sheet. The scatter in individual vortex center location is only slightly affected. However, the average vortex center is now in close agreement with prior AFDD and DLR calculations. The core radius obtained using the planar fit is also in close agreement with other results, and in fact, is a little bit smaller. This suggests that the planar fit would also give accurate results for the peak vorticity and/or the peak swirl velocity.

The vortex core radius and peak swirl velocity are shown as scatter plots in Fig. 16(a) and (b), respectively. At this position, the tip vortex exhibited a moderate aperiodicity magnitude and, therefore, the Devenport correction applied to SA results gave a smaller core radius and larger peak swirl velocity. For the core radius, the corrected SA and the IA results were close to the previous calculations by AFDD, ONERA and DLR reported in [11]. There was a small variation in peak swirl velocity among these different calculations. Contrary to the commonly held belief, the simple average, albeit with the Devenport correction, gave as good results as the other methods. The CA and IA results are also in overall good agreement, and show that the uncertainty in core radius or peak swirl velocity is about 20%. The peak vorticity calculated by different methods is reported in Table 1, where the present results are derived from the Lamb vortex model. The vortex orientation angles are also shown along with similar results from the HART II partners reported in [11].

Another aspect hidden in Figs. 14 and 15 is the uncertainty in vortex center location. As mentioned earlier, the AFDD calculations shown in Ref. [11] used a local method for vortex center based on centroid of vorticity. The ONERA calculations also used a local method based on the centroid of λ_2, while the DLR calculations used a global method based on convolution of λ_2. The uncertainty in vortex center location (that is, the standard deviation in the vortex center location) is shown in Fig. 17 for these different methods along with the planar fit. The distinction between local and global methods is again apparent with the global methods (convolution of λ_2 and the planar least-squares fit) resulting in significantly lower uncertainty.

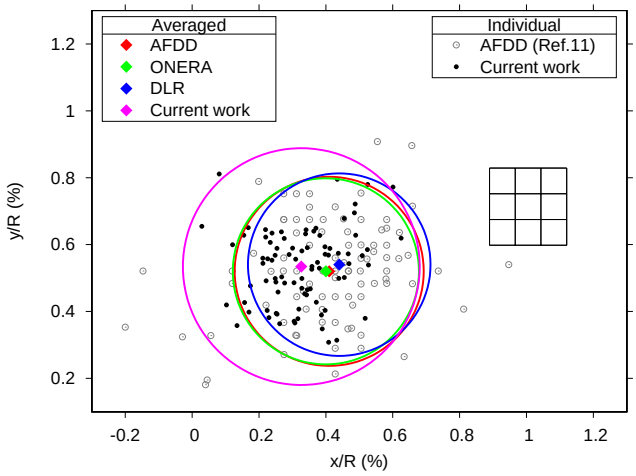

Figure 14: Vortex core size and center locations calculated using the planar fit (with only a single vortex fit to data) for the HART II position 17, along with the results from HART II partners [11]. The large discrepancy observed in the planar fit is a result of fitting a single vortex model to a measured flow field that includes a strong vortex sheet.

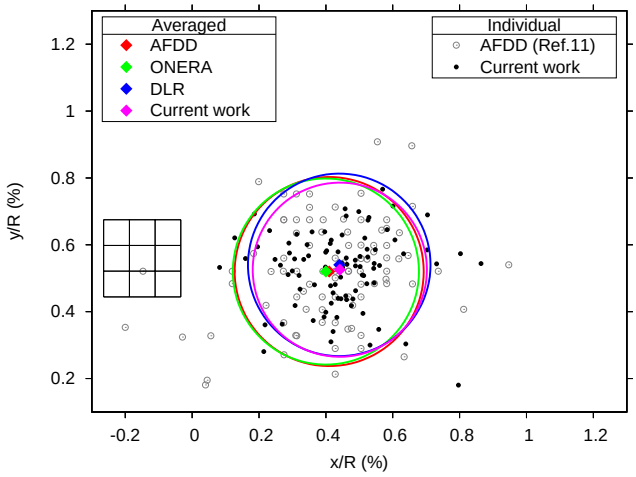

Figure 15: Vortex core for the HART II position 17 calculated using the planar fit modified to include a vortex sheet. The average vortex center location and core size calculated by different HART II partners [11] are also shown for comparison. In addition, the vortex center locations for individual measurements are also shown for the planar fit with those from AFDD in [11].

4. Concluding Remarks

Vortex aperiodicity correction methods can be divided into three general categories: the simple average (SA), the corrected average (CA) or conditional average, and the individual average (IA). The simple average is typically followed by an analytical/empirical correction based on the aperiodicity magnitude. All methods found in literature belong to these categories and differ only in the methods used to determine the vortex properties of interest like vortex center, core radius, peak swirl velocity, etc. These methods are also important because they significantly affect the final perceived measurement uncertainty. Random measurement uncertainty in this context is compared using standard deviation and mean. Global methods that use a larger area of measured data were hypothesized to give less uncertainty in the vortex properties compared to local methods that use only a small subset of data in close to the vortex core. The planar least-squares fit is a global method based on a least-squares fit to a model vortex flow field. This was shown to give a reduced uncertainty in vortex properties like core radius and circulation, and also gave self-consistent results with all three aperiodicity correction methods. The method was also

(a) Vortex core radius

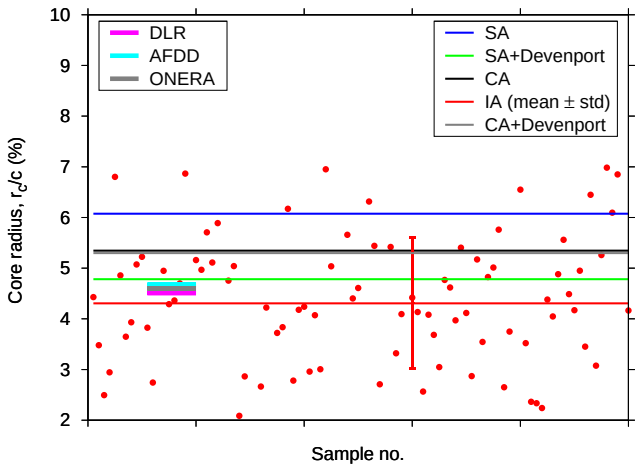

(b) Peak swirl velocity

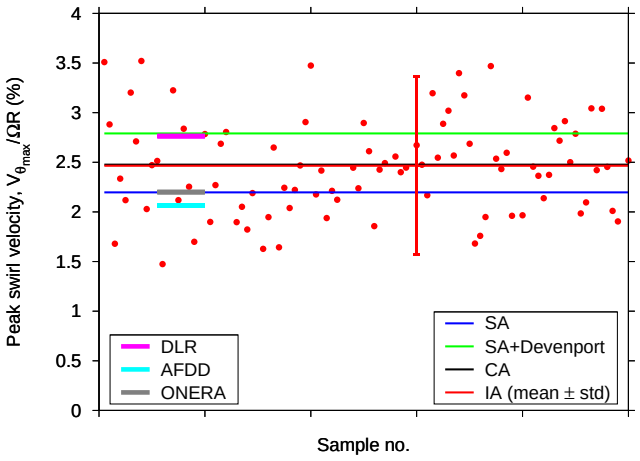

Figure 16: Scatter plots for the vortex properties for HART II position 17 shown with the SA, CA and IA results using the planar fit to include a vortex sheet. Results from the HART II partners reported in [11] are also shown for comparison. (a) Vortex core radius, r_c, (b) Peak swirl velocity, $V_{\theta_{max}}/\Omega R$

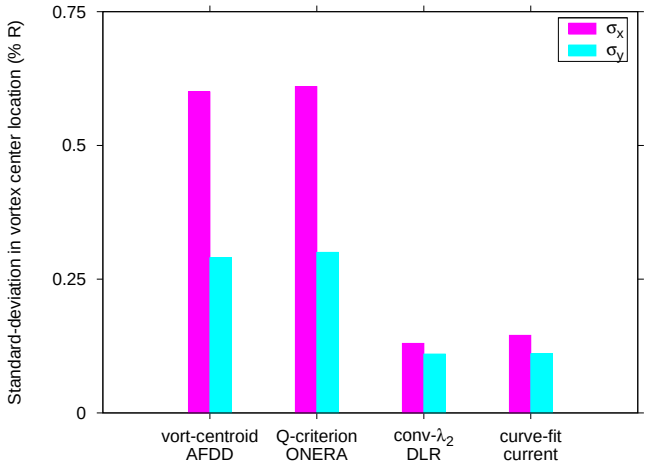

Figure 17: Scatter in vortex center location for individual samples for the HART II position 17. The results using the planar fit are compared with those using different methods in [11].

applied to previous tip vortex measurements for the TRAM and the HART II rotors. In all cases the results showed essentially the same behavior, thus confirming the wide applicability and versatility of this method. Specific conclusions from this study are summarized below.

1. Contrary to commonly held belief, even the simple average, which is both the simplest and the fastest, gave a good estimation of vortex core properties, provided the core radius and peak swirl velocities were corrected using the inverse convolution method developed by Devenport et al. The mean vortex core properties estimated using all three aperiodicity correction methods (SA, CA and IA) were self-consistent and the differences were smaller than half the standard deviation of the individual measurements.
2. The analysis method used to derive vortex properties, like the core radius, plays a significant role in the resulting uncertainty, perhaps a more significant role than the measurement resolution. This was evident from the smallest uncertainty (i.e., the smallest normalized standard deviation) in vortex core radius and circulation for the AFDD model-rotor as compared to other rotor tip vortex PIV measurements. It was hypothesized that global methods, which use all measured data, result in lower uncertainty in the derived vortex properties than local methods, which use only a small sub-set of data close to the vortex core.
3. The AFDD model-rotor measurements were re-analyzed using local method(s) based on horizontal and vertical cuts through the vortex center. These methods showed a higher resultant uncertainty in the vortex core radius and circulation, compared to the global planar fit method. Unlike such straight-line cuts, the results using planar fit were not adversely affected by the lack of valid velocity vectors at the vortex core boundary or by the presence of spurious vectors near the vortex core.
4. The TRAM measurements (both high and low thrust cases) were analyzed using the planar fit, modified to include two vortices. The results showed noticeably lower uncertainty in the derived vortex properties as compared to the previous results using a local method. The results using all three aperiodicity correction methods gave consistent results for both the vortices present in the measured flow field.
5. The HART II measurements at position 17 were also analyzed using the planar fit modified to include a vortex sheet. The results, even the simple average results with the Devenport et al. correction, were consistent with those obtained using different methods by the HART II partners. Furthermore, the planar fit was shown to give accurate vortex center location even in close vicinity of other vortical structures. It was shown that the global methods indeed resulted in smaller uncertainty in vortex center location as compared to the local methods.

References

[1] A. Wadcock, G. K. Yamauchi, E. Solis, A. E. Pete, PIV Measurements in the Wake of a Full-Scale Rotor in Forward Flight, in: 29th AIAA Applied Aerodynamics Conference, Honolulu, HI, 2011.

[2] M. Ramasamy, J. S. Wilson, P. B. Martin, Interaction of Synthetic Jet with Boundary Layer Using Microscopic Particle Image Velocimetry, Journal of Aircraft 47 (2) (2010) 404–422.

[3] M. Ramasamy, R. Paetzel, M. J. Bhagwat, Aperiodicity Correction for Rotor Tip Vortex Measurements, in: Proceedings of the American Helicopter Society 67th Annual National Forum, Virginia Beach, VA, 2010.

[4] M. Ramasamy, J. G. Leishman, Benchmarking Particle Image Velocimetry with Laser Doppler Velocimetry for Rotor Wake Measurements, AIAA Journal 45 (11) (2007) 2622–2633.

[5] G. R. Baker, S. J. Barker, K. K. Bofah, P. G. Saffman, Laser Anemometer Measurements of Trailing Vortices in Water, Journal of Fluid Mechanics 65 (1974) 325–336.

[6] R. K. Takahashi, K. W. McAlister, Preliminary Study of a Wing-Tip Vortex Using Laser Velocimetry, Tech. Rep. TM 88343, NASA (January 1987).

[7] W. J. Devenport, M. C. Rife, S. I. Liapis, G. J. Follin, The Structure and Development of a Wing-Tip Vortex, Journal of Fluid Mechanics 312 (1996) 67–106.

[8] J. G. Leishman, Measurements of the Aperiodic Wake of a Hovering Rotor, Experiments in Fluids 25 (4) (1998) 352–361.

[9] G. K. Yamauchi, C. L. Burley, E. Mercker, K. Pengel, R. JanakiRam, Flow Measurements of an Isolated Model Tilt Rotor, in: Proceedings of the American Helicopter Society 55th Annual National Forum, Montreal, Canada, 1999.

[10] M. Ramasamy, B. Johnson, T. Huismann, J. G. Leishman, A New Method for Estimating Turbulent Vortex Flow Properties from Stereoscopic DPIV Measurements, in: Proceedings of the American Helicopter Society 63rd Annual National Forum, Virginia Beach, VA, 2007.

[11] J. Lim, B. G. van der Wall, An assessment of 3-C PIV analysis methodology for HART II measured data, Tech. Rep. RDMR-AF-10-03, NASA/TM-2010-216024, US Army AFDD (RDECOM) (July 2010).

[12] B. G. van der Wall, H. Richard, Analysis Methodology for 3C-PIV Data of Rotary Wing Vortices, Experiments in Fluids 40 (5) (2006) 798–812.

[13] A. Vogt, P. Baumann, J. Kompenhans, M. Gharib, Investigations of a Wing Tip Vortex in Air by Means of DPIV, in: Proceedings of the 19th AIAA Advanced Measurement and Ground Testing Technology Conference, AIAA-96-2254, New Orleans, LA, 1996.

[14] J. T. Heineck, G. K. Yamauchi, A. J. Wadcock, L. Lourenco, A. I. Abrego, Application of Three-Component PIV to a Hovering Rotor Wake, in: Proceedings of the American Helicopter Society 56th Annual National Forum, Virginia Beach, VA, 2000.

[15] M. Ramasamy, B. Johnson, J. G. Leishman, Turbulent Tip Vortex Measurements Using Dual-Plane Stereoscopic Particle Image Velocimetry, AIAA Journal 47 (8) (2009) 1826–1840.

[16] J. G. Leishman, Seed Particle Dynamics in Tip Vortex Flows, Journal of Aircraft 33 (4) (1996) 823–825.

[17] M. Ramasamy, J. G. Leishman, T. E. Lee, Flow Field of a Rotating Wing MAV, Journal of Aircraft 44 (4) (2007) 1236–1244.

[18] M. J. Bhagwat, J. G. Leishman, Measurements of Bound and Wake Circulation on a Helicopter Rotor, Journal of Aircraft 37 (2) (2000) 227–234.

[19] B. G. Newman, Flow in a Viscous Trailing Vortex, The Aeronautical Quarterly 1 (3) (1959) 167–188.

[20] C. W. Oseen, Über Wirbelbewegung in Einer Reibenden Flüssigkeit, Ark. J. Mat. Astrom. Fys. 7 (1912) 14–21.

[21] H. Lamb, Hydrodynamics, 6th Edition, Cambridge University Press, Cambridge, UK, 1932.

[22] J. D. Iversen, Correlation of Turbulent Trailing Vortex Decay Data, Journal of Aircraft 13 (5) (1976) 338–342.